catalysts

MDPI

Article

Phenolic Acid Decarboxylase for Carbon Dioxide Fixation: Mining, Biochemical Characterization, and Regioselective Enzymatic β-carboxylation of *para*-hydroxystyrene Derivatives

Jie Chen [1], Shirong Wang [1], Junru Zhou [1], Jiaxing Xu [2,*], Bin Wu [1,*], Zhen Gao [1] and Bingfang He [3]

[1] College of Biotechnology and Pharmaceutical Engineering, Nanjing Tech University, 30 Puzhunan Road, Nanjing 211816, China; 202261118054@njtech.edu.cn (J.C.); 202361118014@njtech.edu.cn (S.W.); 202261118058@njtech.edu.cn (J.Z.); gaozhen_njtech@163.com (Z.G.)
[2] College of Chemistry and Chemical Engineering, Huaiyin Normal University, 111 Jiangxi Road, Huai'an 223300, China
[3] School of Pharmaceutical Sciences, Nanjing Tech University, 30 Puzhunan Road, Nanjing 211816, China; bingfanghe@njtech.edu.cn
* Correspondence: xujiaxing@hytc.edu.cn (J.X.); wubin1977@njtech.edu.cn (B.W.)

Abstract: The use of CO_2 as a C1 carbon source for the synthesis of valuable chemicals through biotechnology methods represents an effective strategy to fix carbon dioxide. Phenolic acid decarboxylases possess the capability to introduce a carboxyl group into *para*-hydroxystyrenes for the regionally selective synthesis of (E)-*para*-hydroxycinnamic acids, utilizing bicarbonate as a CO_2 source. It is difficult to achieve this reaction with traditional chemical methods, and only a few enzymes have been isolated and characterized. Here, we mined which low amino acid sequence shared its identity with those of related decarboxylases and which heterologously expressed phenolic acid decarboxylase PAD_Cs from *Clostridium* sp. DSM 8431 in *E. coli*. The recombinant PAD_Cs displayed maximum activity at 50 °C, and pH 5.0. PAD_Cs showed distinct carboxylation ability. The carboxylated substrates have a wide range of substitution modes on aromatic systems, including alkyl and alkoxy groups as well as halogens. Furthermore, the carboxylation conversion rates were impressive: *para*-hydroxystyrene exceeded 20% and 2-methoxy-4-vinylphenol surpassed 26%. This study indicated that PAD_Cs might serve as a potential enzyme source in biotechnological CO_2 fixation.

Keywords: biotechnological CO_2 fixation; enzyme catalysis; phenolic acid (de)carboxylase; *para*-hydroxystyrenes; regioselective carboxylation

check for updates

Academic Editor: Evangelos Topakas

Received: 7 February 2025
Revised: 20 February 2025
Accepted: 21 February 2025
Published: 22 February 2025

Citation: Chen, J.; Wang, S.; Zhou, J.; Xu, J.; Wu, B.; Gao, Z.; He, B. Phenolic Acid Decarboxylase for Carbon Dioxide Fixation: Mining, Biochemical Characterization, and Regioselective Enzymatic β-carboxylation of *para*-hydroxystyrene Derivatives. *Catalysts* **2025**, *15*, 210. https://doi.org/10.3390/catal15030210

Copyright: © 2025 by the authors. Licensee MDPI, Basel, Switzerland. This article is an open access article distributed under the terms and conditions of the Creative Commons Attribution (CC BY) license (https://creativecommons.org/licenses/by/4.0/).

1. Introduction

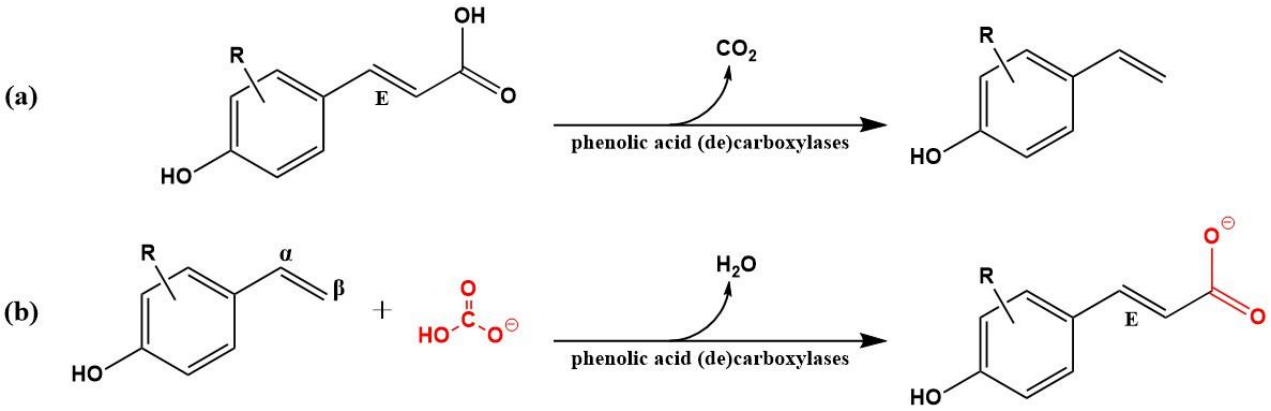
Excessive emissions of carbon have accelerated a series of increasingly serious environmental issues. Moreover, due to its abundant, inexpensive, readily available, and non-toxic nature, carbon dioxide has exhibited great potential in the field of green chemistry and organic synthesis and is an ideal C1 source and carboxylated and carbonylative reagent [1,2]. Therefore, the conversion of CO_2 into useful chemicals has attracted attention [3,4]. To date, researchers have developed strategies such as transition metal catalysis, photocatalysis, electrochemical methods, and enzyme catalysis to achieve the conversion and utilization of carbon dioxide [5–9]. However, the low energetic level of carbon dioxide puts it at a disadvantage in the thermodynamic equilibrium in many chemical processes [5,10]. In addition, the concentration of carbon dioxide in the atmosphere does not allow the direct use of chemical reactions, and the actual reaction of carbon dioxide is often in the form

of bicarbonate in solution, pressurized gas, supercritical state, etc. These unfavorable factors lead to several drawbacks in traditional chemical strategies, such as high costs, low efficiency, significant energy consumption, and adverse environmental impacts. Enzymatic catalysis show mild reaction conditions and a highly regioselective and strong affinity for substrates, providing significant advantages for carbon dioxide utilization.

Carboxylic acids are some of the most important types of compounds in medicinal chemistry and fine chemical synthesis [3]. The direct carboxylation of C-H bonds and CO_2, catalyzed by enzymes, is a more efficient, green, and atomically economical way to produce carboxylic acids. In recent years, some decarboxylases have been reported to have the capacity to introduce a carboxy group in the presence of excess HCO_3^- [8,11]. These (de)carboxylases can be classified into three major categories based on their carboxylation mechanism [12]: (i) Bivalent metal-dependent (de)carboxylases. They all belong to the amidohydrolase superfamily and catalyze the reversible decarboxylation of phenolic acids [13,14]. (ii) Cofactor-independent (de)carboxylases. Phenolic acid decarboxylases are involved in the biodegradation of coumaric acid derivatives [15] and have been able to carboxylate *para*-hydroxystyrene derivatives regioselectively to yield the corresponding (E)-*para*-hydroxycinnamic acids derivatives [16,17]. (iii) prFMN-dependent (de)carboxylases. These enzymes belong to the UbiX-UbiD family. Their catalysis of the diverse reversible decarboxylase reaction relies on the cofactor prenylated FMN [18–21]. Some other (de)carboxylases such as TPP-dependent pyruvate decarboxylase have also been reported to catalyze carboxylation [22].

In the (de)carboxylases described above, phenolic acid decarboxylases do not require any cofactor or metal ion for catalysis, and the reaction they catalyze is non-redox in nature. More importantly, there is a lack of alternative chemical methods for the β-carboxylation of styrene derivatives catalyzed by phenolic acid decarboxylase; only a Pd-catalyzed method for substituted 2-hydroxystryrens has been reported [23]. The main products of β-carboxylation like coumaric acid, ferulic acid, and sinapic acid have multiple biological activities, such as antimicrobial, antioxidant, antiviral, anti-inflammatory, antitumor, antiallergenic, and anti-UV activities [24,25], and are widely used in pharmaceutical, food, cosmetic, and other industries [15]. These advantages have allowed phenolic acid decarboxylase to be regarded as a powerful biocatalytic carboxylation tool [26]. To date, several phenolic acid decarboxylases originating from bacteria or plants have been isolated and characterized for carboxylation [17]. However, the carboxylation catalytic abilities of different phenolic acid decarboxylases vary significantly; for example, the phenolic acid decarboxylase PAD_Ba from *Bacillus amyloliquefaciens* catalyzes the carboxylation of *para*-hydroxystyrene to coumaric acid with a conversion rate of 18%, while PAD_Lp from *Lactobacillus plantarum* achieved only 2% [17]. Therefore, the available sources of phenolic acid decarboxylases remain limited, and their enzymatic properties have yet to be comprehensively investigated. The exploration and development of novel phenolic acid (de)carboxylases continue to hold immense significance.

Searching for homologues to query a sequence with definite activity combined with the vast amount of data available in public databases has massively increased the speed of discovery of enzymes with desired functions [27,28]. In this study, we mined a phenolic acid decarboxylase, named PAD_Cs, from *Clostridium* sp. DSM 8431 through homology sequence searching using PAD_Ba (WP_013353702.1) as the query. This enzyme was able to carboxylate *para*-hydroxystyrene derivatives regioselectively using bicarbonate as the CO_2 source (Scheme 1). We revealed its enzymatic properties and carboxylation performance. Our work provides a new option for the biosynthesis of useful phenolic acid compounds from carbon dioxide.



Scheme 1. Decarboxylation (**a**) and β-carboxylation (**b**) catalyzed by phenolic acid decarboxylase. The red part shows where bicarbonate is involved in the carboxylation reaction as a source of CO_2.

2. Results and Discussion

2.1. Mining of Amino Acid Sequences for (de)Carboxylase

Cofactor-independent phenolic acid decarboxylase is an effective tool to synthesize phenolic acids with biological activity. The lack of alternative chemical methods highlights its unique value. Hitherto, several phenolic acid decarboxylases that can achieve reversible decarboxylation have been reported, such as phenolic acid decarboxylases from *Lactobacillus plantarum* (PAD_Lp), *Bacillus amyloliquefaciens* (PAD_Ba), and ferulic acid decarboxylase from *Enterobacter* sp. (FDC_Es). Among them, PAD_Ba from *Bacillus amyloliquefaciens* is one of the first reported phenolic acid decarboxylases, which can catalyze the reversible decarboxylation of a variety of biologically active phenolic acids such as *p*-coumaric acid, ferulic acid, and erucic acid with a high conversion rate. Therefore, PAD_Ba was utilized as the query in a BLASTp search against the entire NCBI non-redundant (nr) protein database, which returned 3990 sequences. For further screening, we set the Percent Identity to 40–80% and the Query Coverage to 90–99. The similarity threshold was set to 0.9 to remove redundancy from the screened sequences, and about 500 sequences were obtained for the construction of a sequence similarity network (Figure 1). These sequences are roughly clustered into three clusters. Furthermore, 191 sequences clustered in the same cluster as the query sequences were selected to construct the evolutionary tree (Figure S1). We select candidate sequences from the constructed phylogenetic tree based on their proximity to the query sequences. Then, we predict their soluble expression in *E. coli* using Protein–SOL. Finally, several sequences with higher predicted soluble expression values were selected and expressed in *E. coli* using the pET-28a (+) plasmid as the vector. The decarboxylation activity of the crude enzyme was determined for the successfully expressed sequences. The sequence WP_090014602.1 (PAD_Cs) from *Clostridium* sp. DSM 8431 exhibits the highest decarboxylation activity for *p*-coumaric acid, reaching 13.63 IU/mL (The reaction conditions were 50 mM PB buffer with pH 7.0 at 30 °C for 5 min, and the *p*-coumaric acid concentration was 10 mM). Lyophilized cells containing overexpressed enzymes were utilized to verify their carboxylation activity. Under standard carboxylation conditions, the conversion of carboxylated 4-hydroxystyrene in phosphate buffer was measured at 4.04% (no organic cosolvent acetonitrile was added in the reaction system).

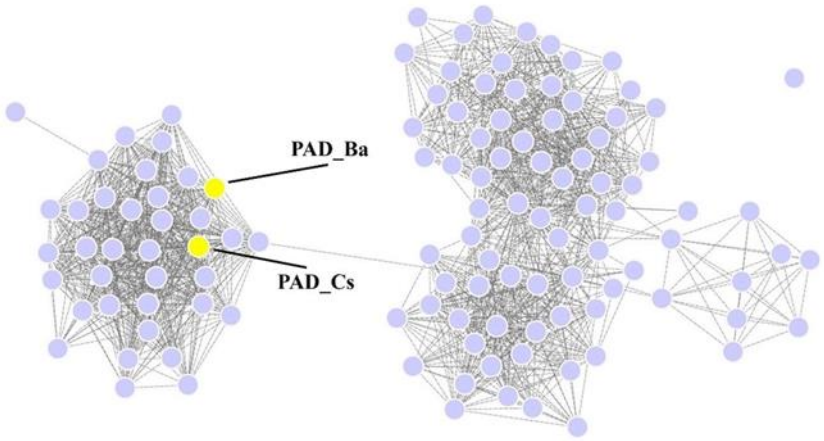


Figure 1. Sequence similarity network (SSN) of phenolic acid decarboxylase protein homologues. Yellow indicates the node where the query PAD_Ba and PAD_Cs are located.

2.2. Sequence Analysis

PAD_Cs from *Clostridium* sp. DSM 8431 consists of 179 amino acids with pI and molecular weight values of 5.1 and 21 kDa, respectively. Sequence analyses show that no secretion signal sequence was found in the amino acid sequence of PAD_Cs. The alignment of the amino acid sequence of PAD_Cs with other phenolic acid decarboxylases that can achieve reversible decarboxylation showed the highest sequence similarities to PAD_Lp from *Lactobacillus plantarum*, PAD_Ll from *Lactoccocus lactis*, PAD_Ba from *Bacillus amyloliquefaciens*, FDC_Es from *Enterobacter* sp., PAD_Mc from *Mycobacterium colombiense*, PAD_Ms from *Methylobacterium* sp., and PAD_Ps from *Pantoea* sp., with 79.8, 76.8, 74.1, 48.2, 47.1, 46.5, and 44.4% identities, respectively. A phylogenetic tree was calculated based on the primary amino acid sequences of PAD_Cs and other reported phenolic acid decarboxylases that can achieve reversible decarboxylation. The phylogenetic tree shows that PAD_Cs and PAD_Lp are closely related (Figure 2).

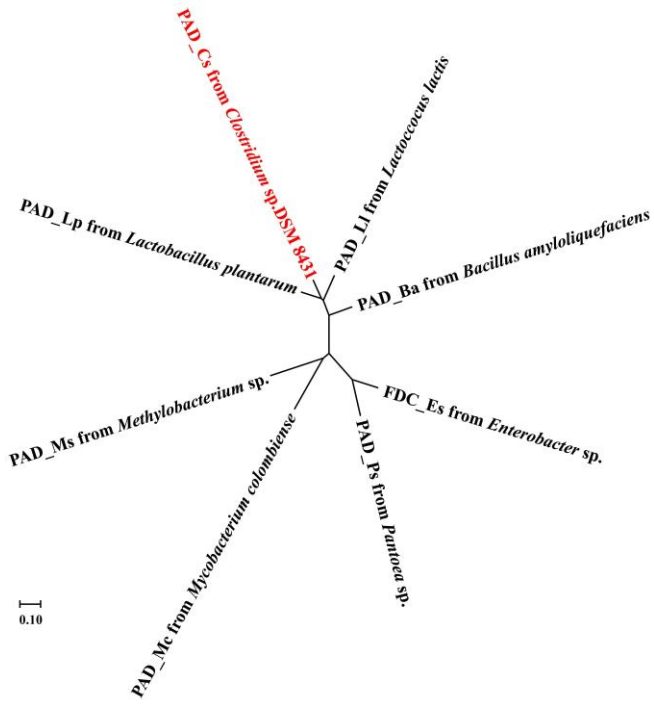


Figure 2. Phylogenetic tree of PAD_Cs and other reported phenolic acid decarboxylases that can achieve reversible decarboxylation. The red part is the enzyme PAD_Cs reported in this work.

2.3. Overexpression and Purification of Recombinant PAD_Cs

Recombinant phenolic acid decarboxylase PAD_Cs was abundantly expressed in *E. coli* with the expression vector pET-28a (+). In order to facilitate the purification of the enzyme, a 6×His-tag was added to the C-end of the sequence. The recombinant PAD_Cs was purified by nickel affinity chromatography following the manufacturer's protocols. The cell debris and supernatant of the cell lysate as well as the purified protein were applied to SDS-PAGE together to determine the molecular mass of the recombinant PAD_Cs. SDS-PAGE showed a strong band of PAD_Cs in the supernatant of the cell lysate. The purified PAD_Cs migrated onto SDS-PAGE as one band with a molecular mass of 21 kDa, the same as the theoretical molecular mass (Figure 3). The larger molecular weight of PAD_Cs, compared to many reported phenolic acid decarboxylases, can be attributed to its longer C-terminal amino acid sequence, which contains approximately 10 additional amino acids. We suspect that this structural difference may contribute to the specific functional properties or regulatory mechanisms of PAD_Cs. The purified PAD_Cs had decarboxylase activity of 175.05 IU/mg for *p*-coumaric acid.

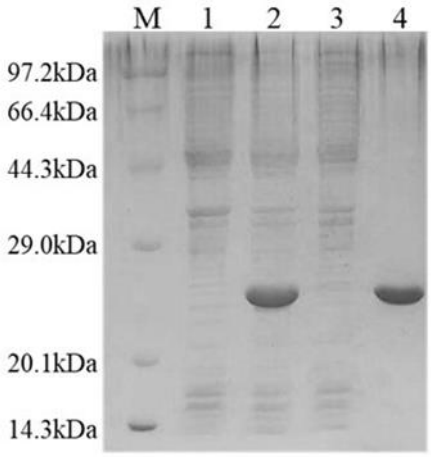


Figure 3. SDS-PAGE analysis of PAD_Cs expressed in *E. coli* BL21 (DE3). Lanes: M, protein molecular weight marker; 1, pET-28a; 2, crude pET-28a- PAD_Cs; 3, purified flow-through; 4, purified pET-28a-PAD_Cs.

2.4. Biochemical and Kinetic Properties of PAD_Cs

The optimal temperature and pH for PAD_Cs were 50 °C and 5.0, respectively. The enzyme also exhibited over 80% relative activity in temperatures ranging from 30 to 55 °C and over 60% in a pH range from 4.5 to 7.0 (Figure 4a,b). Most reported that the optimal temperature of phenolic acid decarboxylase is from 20 to 40 °C, which is much lower than the optimal temperature of PAD_Cs, but the optimal pH of PAD_Cs is similar to that of most reported phenolic acid decarboxylases in the range of 5.0 to 7.0 (Table 1). PAD_Cs was relatively stable at 30 °C, and more than 90% of the activity was retained after 2 h of incubation. However, the enzyme activity rapidly decreased at temperatures above 40 °C (Figure 4c). PAD_Cs was relatively stable at a pH range from 4 to 11 and retained more than 85% of its original activity after 2 h of incubation (Figure 4d). Compared to certain phenolic acid decarboxylases from *L. brevis*, *B. pumilus*, *L. plantarum*, and *Cladosporium phlei*, PAD_Cs exhibits better thermal stability (Table 1). Interestingly, the buffer composition at a pH of 8.0 significantly affected the activity of phenolic acid decarboxylase (PAD_Cs). Specifically, at a solution pH of 8.0, the enzyme activity in the phosphate buffer was significantly lower than that in the Tris-HCl buffer. A similar phenomenon has been observed in several other enzymes, including phenolic acid decarboxylase, α-galactosidase, isocitrate dehydrogenase, and β-N-acetyl glucosaminidase [29–33].

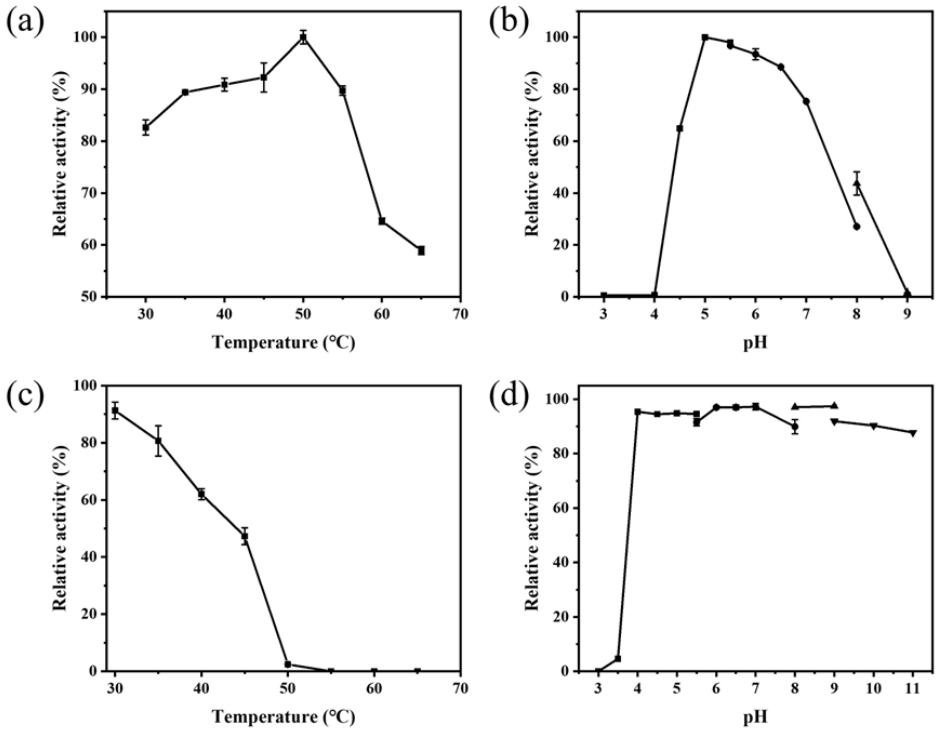


Figure 4. Effects of temperature (**a**) and pH (**b**) on the activity and effects of temperature (**c**) and pH (**d**) on the stability of PAD_Cs.

Table 1. Comparison of the optimum temperature, optimum pH, thermostability, and pH stability of PAD_Cs with other phenolic acid decarboxylases.

Organism	Optimum Temperature (°C)	Optimum pH	Thermostability	pH Stability	Ref
Clostridium sp. DSM 8431	50	5.0	48%, 45 °C, 2 h	>85%, 4–11	This study
Bacillus licheniformis	37	6.0	45%, 45 °C, 1 h	>80%, 5–9	[34]
Lactobacillus brevis RM84	30	6.5	65%, 37 °C, 2 h	NR	[35]
Bacillus pumilus	37	5.5	0%, 42 °C, 30 min	>70%, 5–7	[36]
Lactobacillus plantarum CECT 748^{T}	30	5.0–6.0	1%, 30 °C, 12 h	NR	[37]
Conocephalum japonicum	25	5.5	NR	NR	[38]
Aspergillus luchuensis	40	5.7	100%, 50 °C, 1 h	>80%, 5–10	[39]
Cladosporium phlei	23	6.0	52%, 20 °C, 24 h	NR	[40]

NR: not reported.

The effects of metal ions, surfactants, and organic solvent on PAD_Cs activity were tested by using *p*-coumaric acid as the substrate. The tested metal ions had no or only slight inhibition effects on PAD_Cs activity at concentrations up to 1 mM. Also, at a 1 mM concentration, the surfactant Triton X-100 had a slight stimulatory effect on PAD_Cs activity, but SDS completely inhibited the enzyme activity (Figure 5a). It is worth noting that, unlike SDS, which generally inhibits the activity of phenolic acid decarboxylase, Triton X-100 has significant effects on the activity of various phenolic acid decarboxylase enzymes. For instance, Triton X-100 distinctly inhibits the activity of phenolic acid decarboxylase enzymes from *L. brevis* and *L. plantarum*, while PAD_Cs and the phenolic acid decarboxylase from *Bacillus licheniformis* are activated to varying degrees [34,35,37]. The effects of different organic reagents (10%, *v*/*v*) on enzyme activity showed a significant difference. Polar organic reagents such as methanol and acetonitrile significantly inhibited PAD_Cs activity, while non-polar reagents such as *n*-hexane, petroleum ether, and 1,2 propylene glycol had

fewer detrimental effects on the enzyme activity (Figure 5b). This phenomenon may arise from the immiscibility of n-hexane and petroleum ether with water, resulting in minimal impact on the enzymes within the aqueous phase.

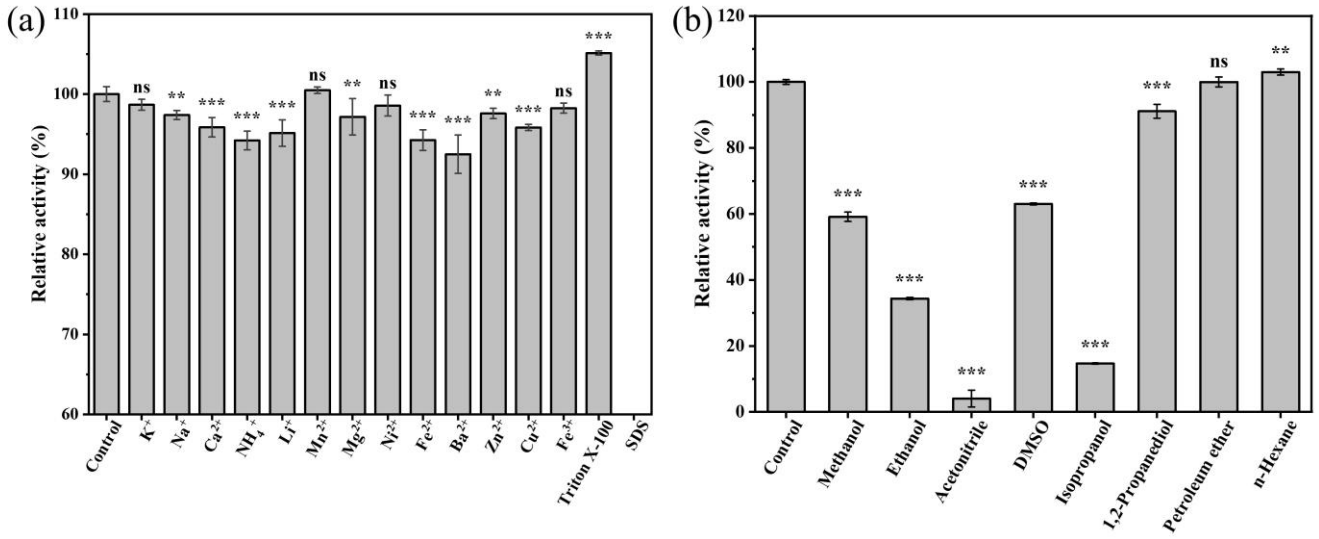


Figure 5. Effect of various metal ions, surfactants (**a**), and organic reagents (**b**) on PAD_Cs activity. The statistical significance of the final results was analyzed using Student's *t*-test, ns: not statistically, ** $p < 0.01$, *** $p < 0.001$.

The kinetic parameters of PAD_Cs were determined using *p*-coumaric acid as the substrate. The kinetic constant K_m value was 8.03 ± 0.50 mM, V_{max} value was 315.53 ± 7.90 IU/mg, K_{cat} value was 50.95 ± 1.28 s^{-1}, and K_{cat}/K_m value was 6.35 ± 0.55 mM^{-1} s^{-1}. Compared with the reported kinetic parameters of phenolic acid decarboxylase, the K_m value of PAD_Cs is larger, the K_{cat} value is smaller, and the K_{cat}/K_m is smaller, which indicates that PAD_Cs has lower catalytic efficiency for the decarboxylation of coumaric acid and a lower affinity for substrates and coumaric acid (Table 2).

Table 2. Comparison of kinetic parameters of PAD_Cs and other phenolic acid decarboxylases.

Organism	Vmax (IU/mg)	K_m (mM)	K_{cat} (s^{-1})	K_{cat}/K_m (mM^{-1} s^{-1})	Ref
Clostridium sp. DSM 8431	315.53 ± 7.90	8.03 ± 0.50	50.95 ± 1.28	6.35 ± 0.55	This study
Bacillus licheniformis	268.43 ± 8.23	1.64 ± 0.12	93.14 ± 2.85	56.75 ± 2.45	[34]
Lactobacillus brevis RM84	9.97	0.98	NR	NR	[35]
Bacillus pumilus	220	1.38	NR	NR	[36]
Lactobacillus plantarum CECT 748^T	711	1.12	NR	NR	[37]
Aspergillus luchuensis	NR	6.63	1122	169.3	[39]
Cladosporium phlei	NR	0.65	NR	NR	[40]

NR: not reported.

2.5. Investigating the β-carboxylation Synthesis Reaction System of p-coumaric Acid by E. coli Whole Cells

Negative controls confirmed the absence of carboxylation activities in empty host cells. Similarly to other phenolic acid decarboxylases capable of achieving reversible decarboxylation, PAD_Cs does not require any cofactors, but still requires a high concentration of bicarbonate (3 M $KHCO_3$) to push the reaction balance toward carboxylation.

The (de)carboxylase PAD_Cs was investigated to catalyze the β-carboxylation of *para*-vinylphenol in a water/acetonitrile system. Unlike most phenolic acid decarboxylases that catalyze reversible decarboxylation, which require acetonitrile with more than 20%

volume fraction in the reaction system, PAD_Cs only requires a lower volume fraction of acetonitrile to achieve a higher *p*-coumaric acid yield [17]. The conversion rate of the reaction initially increases with the volume fraction of acetonitrile, reaching its peak at 12% (Figure 6a, Table 3). However, it then decreases, and no carboxylation activity occurs when the volume fraction of acetonitrile reaches 20%. This indicates that the appropriate concentration of acetonitrile facilitates the dissolution of substrates and products, leading to an improvement in the conversion rate of the reaction. However, a high concentration of acetonitrile causes a rapid loss of enzyme activity. This also suggests that PAD_Cs has a poor tolerance to acetonitrile compared to the reported enzymes.

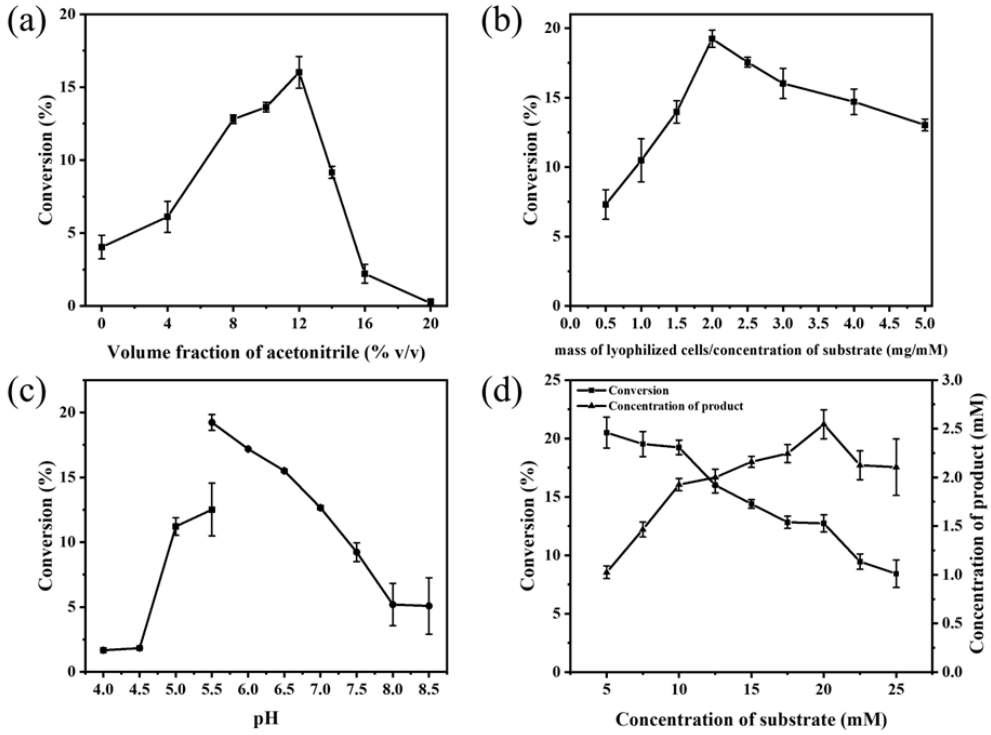


Figure 6. Effects of the volume fraction of acetonitrile (**a**), the ratio of the mass of lyophilized cells to the concentration of substrate (**b**), the pH during the rehydration of lyophilized cells (**c**) and the concentration of substrate (**d**) on the β-carboxylation conversion rate.

Table 3. The conversion rate of PAD_Cs and some reported phenolic acid (de)carboxylases to synthesize bioactive phenolic acid.

Product	Identity (%)	*p*-coumaric Acid	Ferulic Acid	Sinapic Acid
Biocatalyst	**PAD_Cs vs.**	**Conversion (%) [a]**		
PAD_Cs	——	20 [b]	26	3
PAD_Lp	79.8	2 [c]	30	3
PAD_Ll	76.8	3 [c]	2 [c]	4
PAD_Ba	74.1	18 [c]	26 [c]	5

[a] Whole cells of *E. coli* containing overexpressed enzyme. [b] In the presence of 12% acetonitrile (*v*/*v*). [c] In the presence of 20% acetonitrile (*v*/*v*).

The conversion rate was the highest when the ratio of lyophilized cell mass to substrate concentration was 2 (Figure 6b). This suggests that increasing the mass of freeze-dried whole cells in the reaction system does not necessarily increase the conversion rate of the reaction. Too many cells can make the system too sticky and hinder the response. In addition, the addition of excessive bicarbonate will cause the original buffer liquid system to lose its buffering capacity to a certain extent, which can affect the enzyme activity. Therefore,

rehydrating lyophilized whole cells in a buffer with a suitable pH is equally important, as it determines the pH of the final reaction system. Experiments indicate that rehydration exhibits the highest conversion rate at a pH of 5.5 (Figure 6c). It is noteworthy that the carboxylation effect of phosphate buffer surpasses that of citrate buffer at this pH value. We propose that the reason for this phenomenon is similar to the reason that the decarboxylase activity of PAD_Cs in Tris-HCl is higher than that in phosphate buffer at the same pH and buffer concentration. We also investigated the effect of substrate concentration on carboxylation under the condition that the ratio of lyophilized cell mass to substrate concentration was kept constant at 2. The results indicated that the carboxylation conversion rate decreased with the increasing substrate concentration. However, the product concentration initially increased, reaching a peak at a substrate concentration of 20 mM, before decreasing with further increases in the substrate concentration. The carboxylation conversion rate of PAD_Cs for substrate *para*-vinylphenol can reach 20.5%, and the concentration of the product can reach up to 2.55 mM after a 24 h reaction (Figure 6d).

After the optimization of the reaction system, we found that the most suitable carboxylation reaction system (1 mL) for using *para*-vinylphenol as a substrate consisted of the following conditions: lyophilized whole cells were rehydrated in a phosphate buffer of pH 5.5; the final concentration of acetonitrile in the reaction system was 12% (*v*/*v*); 20 mg of lyophilized whole cells, 10 mM substrate, and 300 mg (3 M) $KHCO_3$ were added; and then the mixture was reacted at 30 °C for 24 h. Under these conditions, the conversion rate of the carboxylation reaction is 19.24% and the product concentration is 1.92 mM, which can achieve a better balance between the conversion rate and the product concentration.

2.6. Substrate Scope of the β-carboxylation of para-hydroxystyrenes

The substrate scope of PAD_Cs was studied for the β-carboxylation of *para*-hydroxystyrene derivatives under standard carboxylation conditions (30 mg lyophilized whole cells, 10 mM substrate concentration, and 300 mg $KHCO_3$ were added to 1 mL reaction system). Similarly to other phenolic acid decarboxylases capable of achieving reversible decarboxylation, PAD_Cs tolerated a remarkably broad substitution pattern on the aromatic system. The variety of substituents tolerated in the *meta*-position is rather broad and encompasses alkyl and alkoxy groups as well as halogens. The conversion rate of PAD_Cs to 2-methoxy-4-vinylphenol was observed to be the highest at 26%, indicating a clear preference of PAD_Cs for 2-methoxy-4-vinylphenol in the carboxylation reaction (Figure 7). Compared to the reported enzymes, the conversion rate of carboxylation for substrates other than *para*-hydroxystyrene and 2-methoxy-4-hydroxystyrene was low [17]. Additionally, PAD_Cs demonstrated an inability to carboxylate 2-methyl-4-hydroxystyrene. It is possible that the low solubility of the substrate in the reaction system contributed to this outcome. However, despite these differences, the yields of bioactive compounds such as *p*-coumaric acid, ferulic acid, and erucic acid were in the forefront of similar enzymes (Table 3). We also observed that the concentration of cosolvent acetonitrile required for PAD_Cs to catalyze the carboxylation reaction of different substrates varied significantly. Due to the limitations of enzyme activity, the concentration of the organic cosolvent acetonitrile can only be maintained at a low level. Hence, the organic solvent tolerance of PAD_Cs can be enhanced through protein engineering, immobilized enzymes, and other methods, which is conducive to increasing the substrate concentration of the reaction to improve the conversion rate and yield, so as to achieve preparation-scale applications.

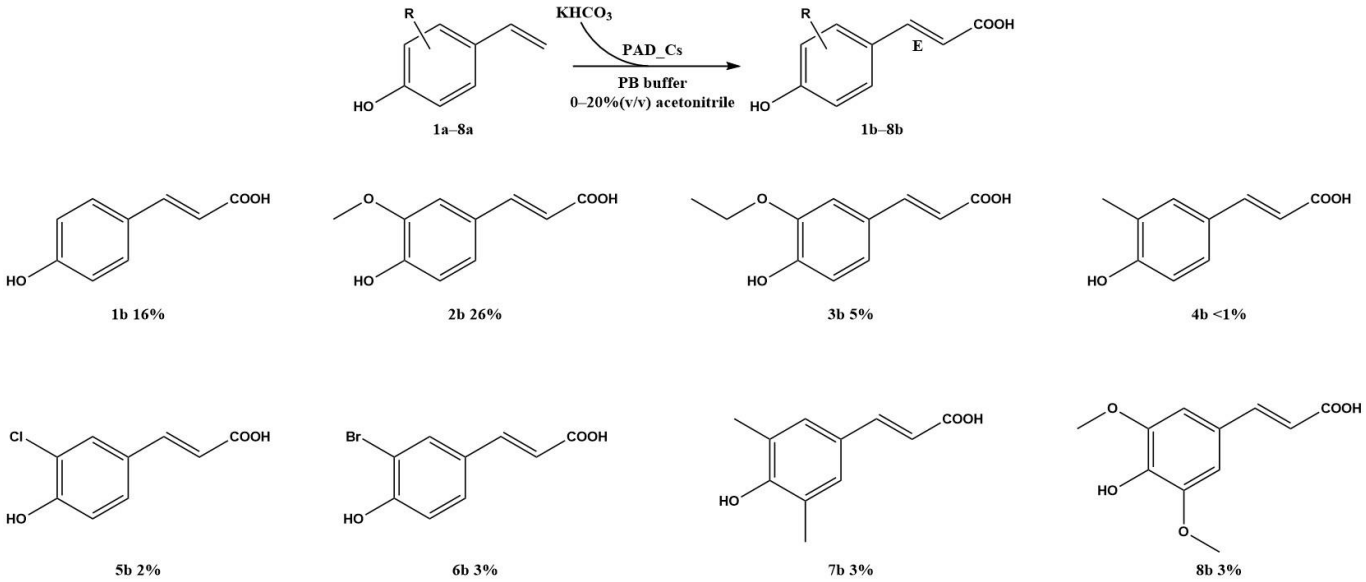


Figure 7. Substrate scope of the β-carboxylation of *para*-hydroxystyrenes.

3. Experimental Procedures

3.1. Materials

The gene encoding for the phenolic acid decarboxylase PAD_Cs was synthesized by Azenta Life Sciences (Suzhou, China). *E. coli* DH5α for gene cloning and *E. coli* BL21 (DE3) and pET-28a (+) for the gene expression of phenolic acid decarboxylases were preserved in our laboratory. 2-Ethoxy-4-vinylphenol (**3a**, 97%), (E)-3-(3-Ethoxy-4-hydroxyphenyl)acrylic acid (**3b**, 97%), 2-Methyl-4-vinylphenol (**4a**, 97%), (E)-3-(4-Hydroxy-3-methylphenyl)acrylic acid (**4b**, 97%), 2-Chloro-4-ethenylphenol (**5a**, 97%), (E)-3-(3-Chloro-4-hydroxyphenyl)acrylic acid (**5b**, 97%), 2-Bromo-4-vinylphenol (**6a**, 97%), (E)-3-(3-Bromo-4-hydroxyphenyl)acrylic acid (**6b**, 97%), 2,6-Dimethyl-4-vinylphenol (**7a**, 97%), and (E)-3-(4-Hydroxy-3,5-dimethylphenyl)acrylic acid (**7b**, 97%) were purchased from Shanghai Medical Technology (Shanghai, China). 4-Hydroxystyrene solution (**1a**, 10% *w*/*w* in propylene glycol), *p*-coumaric acid (**1b**, 98%), 2-Methoxy-4-vinylphenol (**2a**, ≥98%), ferulic acid (**2b**, 99%), and sinapic acid (**8b**, 98%), were purchased from Aladdin Biochemical Technology (Shanghai, China). 2,6-Dimethoxy-4-vinylphenol (**8a**, 97%) was purchased from Bide Pharmatech (Shanghai, China). All other chemicals used were of analytical grade unless otherwise stated.

3.2. Mining and Sequence Analysis of Phenolic Acid (de)carboxylases

The amino acid sequence of reversing decarboxylases PAD_Ba (WP_013353702.1) was used as the query and submitted to a BLASTp search against the entire NCBI nr protein database. The identities of PADs were set within a range of 40–80% identity to search the amino acid sequences. The similarity threshold was set to 0.9 to remove redundancy from the screened sequences, and about 500 sequences were obtained for the further construction of a sequence similarity network (SSN). Additionally, 191 sequences clustered in the same cluster as the query sequences were selected to construct the evolutionary tree. The candidate sequences were selected based on their evolutionary relationship with the query sequences, and predictions were made for their soluble expression in *E. coli*. The heterologously expression of the screened sequences was conducted, and enzyme activity was measured. Sequences exhibiting high enzyme activity were selected to verify whether they possessed carboxylation ability.

Protein homology searches were conducted by BLASTP (https://blast.ncbi.nlm.nih.gov/Blast.cgi, accessed on 9 May 2024). CD-HIT-v4.8.1-2019-0228 was used for the redundancy removal of amino acid sequences [41]. EFI—ENZYME SIMILARITY TOOL (https://efi.igb.illinois.edu/efi-est/, accessed on 9 May 2024) was used for the construction of the sequence similarity network [42]. The phylogenetic tree was constructed using RAxML version 8.2.12. Protein solubility was predicted using a Protein–SOL server (https://protein-sol.manchester.ac.uk/, accessed on 11 May 2024) [43]. The presence of signal peptides was detected using SignalP 5.0 (http://www.cbs.dtu.dk/services/SignalP/, accessed on 11 May 2024) [44]. ClustalW (https://www.genome.jp/tools-bin/clustalw, accessed on 11 May 2024) was used for sequence alignments. The theoretical molecular mass of the recombinant protein was predicted using the ExPASy ProtParam tool (https://web.expasy.org/protparam/, accessed on 11 May 2024).

3.3. Cloning, Overexpression and Purification of Enzymes

The phenolic acid decarboxylase (PAD_Cs) gene (WP_090014602.1) was codon optimized for *E. coli* and synthesized (Azenta Life Sciences, Inc., in Suzhou, China). The phenolic acid decarboxylase gene was amplified using the forward primers (5′-TAACTTTAAGAAGGAGATATACCATGGCGATGAAAAACAAAA-3′ with restriction *Ncol* I site) and reverse primers (5′-TCAGTGGTGGTGGTGGTGGTGCTCGAGTTTAATTTTTTTATA-3′ with restriction *Xho* I site), and then ligated into the corresponding sites of the pET-28a (+) vector. The resulting plasmid was amplified in *E. coli* DH5α, and the inserted gene was verified by DNA sequencing. The plasmid was then introduced into *E. coli* BL21(DE3).

The inoculum was prepared by transferring loopfuls of fresh strains cultured on a Luria broth (LB) agar plate into an LB medium containing kanamycin, followed by incubation at 37 °C for 12 h. The inoculation amount of 2% (*v*/*v*) was transferred to a fresh LB medium containing kanamycin for 4 h at 37 °C and induced with Isopropyl β-D-Thiogalactoside (IPTG) at a final concentration of 0.1 mM at 16 °C for 20 h. The sediment strain of the culture broth was resuspended in 20 mM Tris-HCl buffer (pH 7.5) after centrifugation (12,000 rpm, 4 °C, 10 min) and lysed by ultrasonication on ice (work time: 10 min, work/interval time: 3 s/5 s, and ultrasonic output power: 200 W). The supernatant of total lysate, which was directly used as crude PAD_Cs for purification, was obtained by centrifugation.

The crude PAD_Cs was purified by nickel affinity chromatography following the manufacturer's protocols. Enzyme homogeneity and the molecular weight of purified PAD_Cs were estimated using sodium dodecyl sulfate-polyacrylamide gel electrophoresis (SDS-PAGE) (12% (*w*/*v*)). The protein concentrations were determined using the Bradford method [45].

3.4. Enzyme Assay

p-coumaric acid (10 mM) was incubated with an enzyme sample in 50 mM citrate buffer (pH 5.0) at 50 °C for 5 min (working volume of 1 mL). The reactions were terminated by adding 2 mL acetonitrile. The mixtures were centrifuged (4 °C, 12,000× *g*, 10 min), and the supernatants were subjected to high-performance liquid chromatography (HPLC) analysis. One unit of enzymatic activity was defined as the enzyme required for the production of 1 μmol of 4-vinylphenol per minute.

3.5. Biochemical and Kinetic Properties of PAD_Cs

For the optimal temperature, the enzyme activity was measured at various temperatures (30–65 °C) for 5 min. For optimal pH, the enzyme activity was measured at various pH values (pH 3–11) at 50 °C for 5 min. For estimating the thermostability, the enzyme was pre-incubated at various temperatures and pH 5.0 for 120 min. For estimating the pH

stability, the enzyme was pre-incubated at various pH values (pH 3–11) and at 4 °C for 120 min. Additionally, the 50 mM buffers at each point of pH were as follows: citrate buffer for pH 3–5.5, phosphate buffer for pH 5.5–8, Tris-HCl buffer for pH 8–9, and glycine-NaOH for pH 9–11.

The effects of different metal ions and surfactants on PAD_Cs activity were determined by incubating the enzyme with 1 mM various metal ions or surfactants. The effects of organic solvents on PAD_Cs were determined by incubating the enzyme with various organic solvents in the presence of 10% (v/v).

Kinetic parameters were determined by performing enzymatic reactions at 50 °C, with *p*-coumaric acid (1–20 mM) in 50 mM citrate buffer (pH 5.0) as the substrate. The Origin 2021 software was used for the non-linear regression analysis of the data. The kinetic parameters, i.e., Michaelis constant (K_m), turnover rate (K_{cat}), and catalytic efficiency (K_{cat}/K_m), were obtained by fitting the experimental data to the Michaelis–Menten equation.

3.6. Investigating the β-carboxylation Synthesis Reaction System of p-coumaric Acid by E. coli Whole Cells

The effect of acetonitrile content on carboxylation conversion was determined under standard reaction conditions in different acetonitrile volume fractions from 0 to 20%. The effect of the ratio of the mass of lyophilized cells to the concentration of the substrate was determined under the optimum concentration of acetonitrile. In order to determine the influence of the pH during the rehydration of lyophilized cells on the carboxylation process, lyophilized cells were resuspended in various pH values (pH 4–8.5) before reactions. Additionally, the 100 mM buffers at each point of pH were as follows: citrate buffer for pH 3–5.5, phosphate buffer for pH 5.5–8.5. In order to determine the influence of substrate concentrations, tests were performed by applying increasing amounts of *para*-vinylphenol in the β-carboxylation system ranging from 5 mM to 25 mM under the same ratio of the mass of lyophilized cells to the concentration of the substrate.

3.7. Substrate Specificity in a β-carboxylation Reaction

In order to evaluate the substrate scope of PAD_Cs, structurally diverse compounds differing in the electronic and steric properties were investigated under standard reaction conditions. Post-treatment, the products were evaluated by HPLC. Conversions were determined by comparison with calibration curves for products and substrates prepared with authentic reference material.

3.8. Standard Reaction Conditions and Post-Treatment Procedures for a β-carboxylation Reaction

Carboxylation reactions were performed in glass vials capped with septums. Lyophilized whole cells (30 mg *E. coli* host cells containing the corresponding overexpressed enzyme) were resuspended in phosphate buffer (800 μL, pH 5.5, 100 mM) and were rehydrated by shaking at 600 rpm at 30 °C for 30 min. The substrate was added either directly or from a stock solution to yield a final concentration of 10 mM, followed by the addition of acetonitrile (0–20% v/v, 200 μL) and $KHCO_3$ (3 M, 300 mg). The vials were tightly closed, and the mixture was shaken at 30 °C and 600 rpm for 24 h. Thereafter, the mixture was centrifuged (13,000 rpm, 15 min) and an aliquot of 100 μL was diluted with 1 mL of an H_2O/acetonitrile mixture (v/v 1:1) supplemented with trifluoroacetic acid (3% v/v, 30 μL). After incubation at room temperature for 5 min, the samples were recentrifuged (13,000 rpm, 15 min) and the conversions were analyzed on a reverse-phase HPLC. Products were identified by comparison with authentic reference material. Empty host cells were used as negative controls.

3.9. Analytical Procedures

All liquid chromatography measurements were carried out using an Agilent HPLC (Model-1200, reverse phase) equipped with a C18 (Agilent 5 HC-C18, 250 × 4.6 mm, 5 μm). The method was run over 10 min with H_2O/TFA (0.1%) and MeCN/TFA (0.1%) in different proportions as the mobile phase at a flow rate of 1 mL min^{-1} (detailed mobile phase conditions are provided in the Supplementary Material). The column temperature was 24 °C, and the compounds were spectrophotometrically detected at dual wavelengths. All carboxylation products were further confirmed by anion mass spectrometry. To avoid interference from other substances in the reaction system, we chose detection at 320 nm ultraviolet wavelength as the analysis basis for the carboxylation reaction, where the main response signal comes from the products of the carboxylation reaction.

3.10. Statistical Analysis

Experiments were conducted with at least three biological replicates, and results are displayed as the mean ± standard deviation. Statistical analyses were conducted using GraphPad Prism 9 software, and figures were created with Origin 2021 software.

4. Conclusions

In conclusion, we successfully mined and heterologously expressed a phenolic acid decarboxylase PAD_Cs from *Clostridium* sp. DSM 8431; it can introduce the carboxy group into *para*-hydroxystyrene derivatives to yield the corresponding (E)-*para*-hydroxycinnamic acids at the expense of using bicarbonate as the CO_2 source. We investigated its enzymatic properties and carboxylation performance. PAD_Cs showed distinct carboxylation ability, the carboxylation conversion rate of *para*-hydroxystyrene reached more than 20%, and 2-methoxy-4-vinylphenol reached more than 26%. This offers a promising avenue for utilizing carbon dioxide to generate bioactive phenolic acids in an environmentally sustainable and large-scale manner.

Supplementary Materials: The following supporting information can be downloaded at https://www.mdpi.com/article/10.3390/catal15030210/s1, Figure S1: Evolutionary tree of sequences consistent with template sequence clustering; Figure S2: Multiple sequence alignment of PAD_Cs and other reported phenolic acid decarboxylases that can achieve reversible decarboxylation; Figures S3–S9: The HPLC and MS spectrometry detection spectra of the carboxylation reaction products; Figure S10: Kinetic curve fitting of PAD_Cs. The detailed HPLC mobile phase and UV detection conditions are also described in the Supplementary Materials.

Author Contributions: Conceptualization, J.C. and B.W.; data curation, J.C. and S.W.; funding acquisition, J.X. and B.W.; investigation, J.Z., Z.G. and B.H.; writing—original draft, J.C.; writing—review and editing, J.X. and B.W. All authors have read and agreed to the published version of the manuscript.

Funding: This research was funded by the National Natural Science Foundation of China (22478189), General Programs of the National Natural Science Foundation of China (22078122).

Data Availability Statement: All data included in this study are available from the corresponding author by request.

Acknowledgments: The computational resources generously provided by the High Performance Computing Center of Nanjing Tech University are greatly appreciated.

Conflicts of Interest: The authors declare that they have no competing financial interest.

References

1. Cai, X.; Xie, B. Direct Carboxylative Reactions for the Transformation of Carbon Dioxide into Carboxylic Acids and Derivatives. *Synthesis* **2013**, *45*, 3305–3324. [CrossRef]
2. Wang, L.; Sun, W.; Liu, C. Recent Advances in Homogeneous Carbonylation Using CO_2 as CO Surrogate. *Chin. J. Chem.* **2018**, *36*, 353–362. [CrossRef]
3. Zhang, Z.; Muschiol, J.; Huang, Y.; Sigurdardóttir, S.B.; von Solms, N.; Daugaard, A.E.; Wei, J.; Luo, J.; Xu, B.-H.; Zhang, S.; et al. Efficient ionic liquid-based platform for multi-enzymatic conversion of carbon dioxide to methanol. *Green Chem.* **2018**, *20*, 4339–4348. [CrossRef]
4. Wang, S.; Xu, M.; Peng, T.; Zhang, C.; Li, T.; Hussain, I.; Wang, J.; Tan, B. Porous hypercrosslinked polymer-TiO_2-graphene composite photocatalysts for visible-light-driven CO_2 conversion. *Nat. Commun.* **2019**, *10*, 676. [CrossRef] [PubMed]
5. Ishida, N.; Shimamoto, Y.; Murakami, M. Solar-Driven Incorporation of Carbon Dioxide into α-Amino Ketones. *Angew. Chem. Int. Ed.* **2012**, *51*, 11750–11752. [CrossRef]
6. Song, J.; Liu, Q.; Liu, H.; Jiang, X. Recent Advances in Palladium-Catalyzed Carboxylation with CO_2. *Eur. J. Org. Chem.* **2018**, *2018*, 696–713. [CrossRef]
7. Senboku, H. Electrochemical Fixation of Carbon Dioxide: Synthesis of Carboxylic Acids. *Chem. Rec.* **2021**, *21*, 2354–2374. [CrossRef] [PubMed]
8. Bierbaumer, S.; Nattermann, M.; Schulz, L.; Zschoche, R.; Erb, T.J.; Winkler, C.K.; Tinzl, M.; Glueck, S.M. Enzymatic Conversion of CO_2: From Natural to Artificial Utilization. *Chem. Rev.* **2023**, *123*, 5702–5754. [CrossRef] [PubMed]
9. Roger, M.; Reed, T.C.P.; Sargent, F.; Semrau, J.D. Harnessing Escherichia coli for Bio-Based Production of Formate under Pressurized H_2 and CO_2 Gases. *Appl. Environ. Microbiol.* **2021**, *87*, e00299-21. [CrossRef] [PubMed]
10. Müller, K.; Mokrushina, L.; Arlt, W. Thermodynamic Constraints for the Utilization of CO_2. *Chem. Ing. Tech.* **2014**, *86*, 497–503. [CrossRef]
11. Kino, K.; Hirokawa, Y.; Gawasawa, R.; Murase, R.; Tsuchihashi, R.; Hara, R. Screening, gene cloning, and characterization of orsellinic acid decarboxylase from Arthrobacter sp. K8 for regio-selective carboxylation of resorcinol derivatives. *J. Biotechnol.* **2020**, *323*, 128–135. [CrossRef] [PubMed]
12. Payer, S.E.; Faber, K.; Glueck, S.M. Non-Oxidative Enzymatic (De)Carboxylation of (Hetero)Aromatics and Acrylic Acid Derivatives. *Adv. Synth. Catal.* **2019**, *361*, 2402–2420. [CrossRef] [PubMed]
13. Seibert, C.M.; Raushel, F.M. Structural and Catalytic Diversity within the Amidohydrolase Superfamily. *Biochemistry* **2005**, *44*, 6383–6391. [CrossRef] [PubMed]
14. Kirimura, K.; Gunji, H.; Wakayama, R.; Hattori, T.; Ishii, Y. Enzymatic Kolbe–Schmitt reaction to form salicylic acid from phenol: Enzymatic characterization and gene identification of a novel enzyme, Trichosporon moniliiforme salicylic acid decarboxylase. *Biochem. Biophys. Res. Commun.* **2010**, *394*, 279–284. [CrossRef]
15. Tinikul, R.; Chenprakhon, P.; Maenpuen, S.; Chaiyen, P. Biotransformation of Plant-Derived Phenolic Acids. *Biotechnol. J.* **2018**, *13*, 1700632. [CrossRef] [PubMed]
16. Wuensch, C.; Glueck, S.M.; Gross, J.; Koszelewski, D.; Schober, M.; Faber, K. Regioselective Enzymatic Carboxylation of Phenols and Hydroxystyrene Derivatives. *Org. Lett.* **2012**, *14*, 1974–1977. [CrossRef] [PubMed]
17. Wuensch, C.; Pavkov-Keller, T.; Steinkellner, G.; Gross, J.; Fuchs, M.; Hromic, A.; Lyskowski, A.; Fauland, K.; Gruber, K.; Glueck, S.M.; et al. Regioselective Enzymatic β-Carboxylation of para-Hydroxy- styrene Derivatives Catalyzed by Phenolic Acid Decarboxylases. *Adv. Synth. Catal.* **2015**, *357*, 1909–1918. [CrossRef]
18. Payne, K.A.P.; White, M.D.; Fisher, K.; Khara, B.; Bailey, S.S.; Parker, D.; Rattray, N.J.W.; Trivedi, D.K.; Goodacre, R.; Beveridge, R.; et al. New cofactor supports α,β-unsaturated acid decarboxylation via 1,3-dipolar cycloaddition. *Nature* **2015**, *522*, 497–501. [CrossRef] [PubMed]
19. Bloor, S.; Michurin, I.; Titchiner, G.R.; Leys, D. Prenylated flavins: Structures and mechanisms. *FEBS J.* **2022**, *290*, 2232–2245. [CrossRef] [PubMed]
20. Marshall, S.A.; Payne, K.A.P.; Leys, D. The UbiX-UbiD system: The biosynthesis and use of prenylated flavin (prFMN). *Arch. Biochem. Biophys.* **2017**, *632*, 209–221. [CrossRef] [PubMed]
21. Heker, I.; Haberhauer, G.; Meckenstock, R.U. Naphthalene Carboxylation in the Sulfate-Reducing Enrichment Culture N47 Is Proposed to Proceed via 1,3-Dipolar Cycloaddition to the Cofactor Prenylated Flavin Mononucleotide. *Appl. Environ. Microbiol.* **2023**, *89*, e0192722. [CrossRef] [PubMed]
22. Miyazaki, M.; Shibue, M.; Ogino, K.; Nakamura, H.; Maeda, H. Enzymatic synthesis of pyruvic acid from acetaldehyde and carbon dioxide. *Chem. Commun.* **2001**, *18*, 1800–1801. [CrossRef]
23. Sasano, K.; Takaya, J.; Iwasawa, N. Palladium(II)-Catalyzed Direct Carboxylation of Alkenyl C-H Bonds with CO_2. *J. Am. Chem. Soc.* **2013**, *135*, 10954–10957. [CrossRef] [PubMed]
24. Ou, S.; Kwok, K.C. Ferulic acid: Pharmaceutical functions, preparation and applications in foods. *J. Sci. Food Agric.* **2004**, *84*, 1261–1269. [CrossRef]

25. Roychoudhury, S.; Sinha, B.; Choudhury, B.P.; Jha, N.K.; Palit, P.; Kundu, S.; Mandal, S.C.; Kolesarova, A.; Yousef, M.I.; Ruokolainen, J.; et al. Scavenging Properties of Plant-Derived Natural Biomolecule Para-Coumaric Acid in the Prevention of Oxidative Stress-Induced Diseases. *Antioxidants* **2021**, *10*, 1205. [CrossRef] [PubMed]
26. Sheng, X.; Himo, F. Theoretical Study of Enzyme Promiscuity: Mechanisms of Hydration and Carboxylation Activities of Phenolic Acid Decarboxylase. *ACS Catal.* **2017**, *7*, 1733–1741. [CrossRef]
27. Cui, L.; Cui, A.; Li, Q.; Yang, L.; Liu, H.; Shao, W.; Feng, Y. Molecular Evolution of an Aminotransferase Based on Substrate–Enzyme Binding Energy Analysis for Efficient Valienamine Synthesis. *ACS Catal.* **2022**, *12*, 13703–13714. [CrossRef]
28. Kelly, S.A.; Mix, S.; Moody, T.S.; Gilmore, B.F. Transaminases for industrial biocatalysis: Novel enzyme discovery. *Appl. Microbiol. Biotechnol.* **2020**, *104*, 4781–4794. [CrossRef]
29. Wang, J.; Cao, X.; Chen, W.; Xu, J.; Wu, B. Identification and Characterization of a Thermostable GH36 α-Galactosidase from Anoxybacillus vitaminiphilus WMF1 and Its Application in Synthesizing Isofloridoside by Reverse Hydrolysis. *Int. J. Mol. Sci.* **2021**, *22*, 10778. [CrossRef] [PubMed]
30. Huang, Z.; Zhou, J.; Wang, J.; Xu, S.; Cheng, C.; Ma, J.; Gao, Z. Complementary Distant and Active Site Mutations Simultaneously Enhance Catalytic Activity and Thermostability of α-Galactosidase. *J. Agric. Food Chem.* **2025**, *73*, 3635–3644. [CrossRef]
31. Huang, H.-K.; Tokashiki, M.; Maeno, S.; Onaga, S.; Taira, T.; Ito, S. Purification and properties of phenolic acid decarboxylase from Candida guilliermondii. *J. Ind. Microbiol. Biotechnol.* **2012**, *39*, 55–62. [CrossRef]
32. Wang, X.; Tang, X.; Chen, H.; Zhang, H.; Chen, Y.Q.; Zhao, J.; Chen, W. Purification and characterization of isocitrate dehydrogenase from Mortierella alpina. *Process Biochem.* **2022**, *121*, 575–583. [CrossRef]
33. Zhang, A.; Mo, X.; Zhou, N.; Wang, Y.; Wei, G.; Chen, J.; Chen, K.; Ouyang, P. A novel bacterial β-N-acetyl glucosaminidase from *Chitinolyticbacter meiyuanensis* possessing transglycosylation and reverse hydrolysis activities. *Biotechnol. Biofuels* **2020**, *13*, 115. [CrossRef]
34. Hu, H.; Li, L.; Ding, S. An organic solvent-tolerant phenolic acid decarboxylase from Bacillus licheniformis for the efficient bioconversion of hydroxycinnamic acids to vinyl phenol derivatives. *Appl. Microbiol. Biotechnol.* **2014**, *99*, 5071–5081. [CrossRef]
35. Landete, J.M.; Rodríguez, H.; Curiel, J.A.; de las Rivas, B.; Mancheño, J.M.; Muñoz, R. Gene cloning, expression, and characterization of phenolic acid decarboxylase from Lactobacillus brevis RM84. *J. Ind. Microbiol. Biotechnol.* **2010**, *37*, 617–624. [CrossRef] [PubMed]
36. Degrassi, G.; Polverino De Laureto, P.; Bruschi, C.V. Purification and Characterization of Ferulate and *p*-Coumarate Decarboxylase from *Bacillus pumilus*. *Appl. Environ. Microbiol.* **1995**, *61*, 326–332. [CrossRef]
37. RODRiguez, H.; Landete, J.M.; Curiel, J.A.; de Las Rivas, B.; Mancheño, J.M.; Muñoz, R. Characterization of the *p*-coumaric Acid Decarboxylase from Lactobacillus plantarum CECT 748. *J. Agric. Food Chem.* **2008**, *56*, 3068–3072. [CrossRef] [PubMed]
38. Gao, S.; Yu, H.-N.; Wu, Y.-F.; Liu, X.-Y.; Cheng, A.-X.; Lou, H.-X. Cloning and functional characterization of a phenolic acid decarboxylase from the liverwort Conocephalum japonicum. *Biochem. Biophys. Res. Commun.* **2016**, *481*, 239–244. [CrossRef] [PubMed]
39. Maeda, M.; Tokashiki, M.; Tokashiki, M.; Uechi, K.; Ito, S.; Taira, T. Characterization and induction of phenolic acid decarboxylase from Aspergillus luchuensis. *J. Biosci. Bioeng.* **2018**, *126*, 162–168. [CrossRef]
40. Harada, T.; Mino, Y. Some properties of *p*-coumarate decarboxylase from *Cladosporium phlei*. *Can. J. Microbiol.* **1976**, *22*, 1258–1262. [CrossRef] [PubMed]
41. Fu, L.; Niu, B.; Zhu, Z.; Wu, S.; Li, W. CD-HIT: Accelerated for clustering the next-generation sequencing data. *Bioinformatics* **2012**, *28*, 3150–3152. [CrossRef] [PubMed]
42. Rodríguez Benítez, A.; Narayan, A.R.H. Frontiers in Biocatalysis: Profiling Function across Sequence Space. *ACS Cent. Sci.* **2019**, *5*, 1747–1749. [CrossRef]
43. Hebditch, M.; Carballo-Amador, M.A.; Charonis, S.; Curtis, R.; Warwicker, J.; Valencia, A. Protein–Sol: A web tool for predicting protein solubility from sequence. *Bioinformatics* **2017**, *33*, 3098–3100. [CrossRef]
44. Almagro Armenteros, J.J.; Tsirigos, K.D.; Sønderby, C.K.; Petersen, T.N.; Winther, O.; Brunak, S.; von Heijne, G.; Nielsen, H. SignalP 5.0 improves signal peptide predictions using deep neural networks. *Nat. Biotechnol.* **2019**, *37*, 420–423. [CrossRef] [PubMed]
45. Bradford, M.M. A rapid and sensitive method for the quantitation of microgram quantities of protein utilizing the principle of protein-dye binding. *Anal. Biochem.* **1976**, *72*, 248–254. [CrossRef]

Disclaimer/Publisher's Note: The statements, opinions and data contained in all publications are solely those of the individual author(s) and contributor(s) and not of MDPI and/or the editor(s). MDPI and/or the editor(s) disclaim responsibility for any injury to people or property resulting from any ideas, methods, instructions or products referred to in the content.